Mansour, T. E. (1970), *Advan. Enzyme Regul. 8*, 37.
Mathias, M. M., and Kemp, R. G. (1972), *Biochemistry 11*, 578.
Murphy, A. J., Duke, J. A., and Stowring, L. (1970), *Arch. Biochem. Biophys. 137*, 297.
Paetkau, V., and Lardy, H. A. (1967), *J. Biol. Chem. 242*, 2035.
Paetkau, V. H., Younathan, E. S., and Lardy, H. A. (1968), *J. Mol. Biol. 33*, 721.
Parmeggiani, A., and Bowman, R. H. (1963), *Biochem. Biophys. Res. Commun. 12*, 268.
Parmeggiani, A., Luft, J. H., Love, D. S., and Krebs, E. G. (1966), *J. Biol. Chem. 241*, 4625.
Passoneau, J. V., and Lowry, O. H. (1962), *Biochem. Biophys. Res. Commun. 7*, 10.
Santos, E. C., and Spector, A. A. (1972), *Biochemistry 11*, 2299.
Seery, V. L., and Anderson, S. R. (1972), *Biochemistry 11*, 707.
Stryer, L. (1965), *J. Mol. Biol. 13*, 482.
Thompson, W., and Yielding, K. L. (1968), *Arch. Biochem. Biophys. 126*, 399.
Turner, D. C., and Brand, L. (1968), *Biochemistry 7*, 3381.
Uyeda, K., and Racker, E. (1965), *J. Biol. Chem. 240*, 4682.
Weber, G., and Daniel, E. (1966), *Biochemistry 5*, 1900.
Weber, G., and Young, L. B. (1964), *J. Biol. Chem. 239*, 1415.
Younathan, E. S., Paetkau, V., and Lardy, H. A. (1968), *J. Biol. Chem. 243*, 1603.

Chemical Kinetic and Proton Magnetic Resonance Studies of 5′-Adenosine Monophosphate Binding to Ribonuclease A†

Peter H. Haffner* and Jui H. Wang‡

ABSTRACT: The effects of 5′-AMP on the kinetics of ribonuclease A catalyzed hydrolysis of cyclic CMP have been analyzed. The results suggest the existence of the ternary complex, enzyme–cyclic CMP–5′-AMP, which breaks down to product approximately three times faster than the enzyme–cyclic CMP complex at pH 5.57. The pH profile for the binding constant of 5′-AMP to ribonuclease A has been determined in the pH range 4–8.5. The shape of this profile is very similar to that found previously for the binding of orthophosphate and 3′-pyrimidine nucleotides to the enzyme. The titration curves of the individual histidine residues of ribonuclease A have been determined by measuring the pD dependence of the proton magnetic resonance chemical shifts of the imidazole C-2 proton resonance for each histidine. The shapes of the His-12 and His-119 curves were found to be abnormal in the pH region 3–5.2. These results call into question the assignments of the His-12 and His-119 resonance lines, but a linewidth analysis of these two resonances over the entire pD region has substantiated the originally proposed assignments. The abnormal shape of these two titration curves demonstrates a change in the environment of both His-12 and His-119 which accompanies the titration to low pD. The effects of 5′-AMP binding on the aromatic region of the ribonuclease A nuclear magnetic resonance (nmr) spectrum have been observed over the pD range 3–8.5. 5′-AMP binding perturbs the pK_a values of His-12 and -119 from their free enzyme values of 6.2 and 6.06 to 7.6 and 6.3, respectively. In addition, the His-119 resonance is shifted upfield some 20 Hz at low pD. The presence of 5′-AMP has no observable effect on the large Phe-120 peak associated with the pyrimidine nucleotide binding pocket at the enzyme surface. The results demonstrate that the phosphate moiety of 5′-AMP is bound at the same site on the enzyme surface at which the phosphate of 3′-pyrimidine nucleotide is bound. In contrast to the 3′-pyrimidine nucleotide case, there is only a very weak interaction between the phosphate of bound 5′-AMP and His-119. Like pyrimidine nucleotide, 5′-AMP phosphate has a strong acid stabilizing influence on His-12. The shielding effect on the fully protonated His-119 resonance at low pD is consistent with a base stacking interaction between the adenine ring of bound 5′-AMP and the imidazole ring of His-119.

Bovine pancreatic ribonuclease A catalyzes the hydrolysis of RNA and (3′,5′)-dinucleoside phosphate esters in two steps. The first step is an intramolecular transesterification to a stable (2′,3′) cyclic phosphate intermediate which is, in turn, hydrolyzed to a 3′-nucleotide (Brown and Todd, 1953; Brocklehurst *et al.*, 1967). Recently, X-ray crystallographic studies (Carlson, W. D., *et al.*, to be published) of ribonuclease S, a proteolytically modified derivative of ribonuclease A, have uncovered an adenosine nucleotide binding site at the enzyme surface. This site is directly adjacent to the site occupied by bound pyrimidine nucleotide and presumably by poly- and (2′,3′) cyclic pyrimidine nucleotide substrates as well. Previously, substrate specificity studies had revealed that in the ribonuclease A catalyzed transesterification of (3′,5′)-dinucleoside phosphate esters, the enzyme exhibits a marked preference for purine, particularly adenosine, as the 5′ alcohol (Witzel and Barnard, 1962; Gassen and Witzel,

† From the Department of Chemistry, Yale University, New Haven, Connecticut 06510. *Received October 26, 1972.* This material was submitted by P. H. H. to the Graduate School of Yale University in partial fulfillment of the requirements for the Ph.D. degree. This work was supported by research grants from the National Institute of General Medical Sciences (GM 044 83 and GM 19990-01) and a Public Health Service Training grant (00748-09).

* Present address: Department of Molecular Biophysics and Biochemistry, Yale University.

‡ Present address: Bioenergetics Lab, State University of New York at Buffalo, Buffalo, New York 14214.

1967). Also, Wieker and Witzel (1967) had found that adenine, adenosine, (3′,5′) cyclic AMP,[1] and (3′,5′)-adenosyladenosine all stimulate ribonuclease activity during (2′,3′) cyclic CMP[1] hydrolysis.

Richards and Wyckoff (1971) have described the structures of several enzyme–inhibitor complexes. The complex which best simulates an actual enzyme–substrate complex is that with UpcA,[1] an inactive phosphonate analog of UpA.[1] The respective sites at the enzyme surface for UpcA binding have been designated as B_1, R_1, p_1, R_2, and B_2 for the uridine base, the uridine ribose, the phosphonate, the adenosine ribose, and the adenine base. In mononucleotide binding, 3′-CMP occupies $B_1R_1p_1$, while 5′-AMP occupies $p_1R_2B_2$. The results of the crystallographic studies to date suggest that the active-site conformation is different for different bound ligands (Richards and Wyckoff, 1971). This conformational change involves His-119, a residue suspected to play an important role in catalysis. While the position of His-119 is not clearly defined in the free enzyme, there seem to be at least four positions, designated I, II, III, and IV by Richards and Wyckoff, that His-119 may occupy. With UpcA or adenosine mononucleotide bound, His-119 seems to be stabilized in position IV in which the adenine ring is stacked on the His-119 with imidazole N_3 close enough to Asp-121 for possible interaction with the carboxyl. That position IV is a proper configuration for catalysis of transesterification is suggested by the strong similarity between UpcA and the real substrate.

With 3′-CMP bound, position III seems to be somewhat stabilized. Position III is close to the R_2 site, and there is little doubt that position III is catalytically abortive at least for catalysis of step I transesterification.

Using chemical kinetic and proton magnetic resonance (pmr) techniques, we have attempted to uncover further detail about the adenosine binding site, the His-119 configurational equilibrium, and their relation to the activation of the enzyme by adenosine derivatives. Pmr has proven to be a powerful tool in elucidating structural details of the pyrimidine nucleotide binding site, B_1R_1 (Meadows and Jardetsky, 1969; Meadows *et al.*, 1969; Ruterjans and Witzel, 1969). The method has also uncovered interactions between amino acid residues at the active site of the free enzyme (Ruterjans and Witzel, 1969; Haffner, 1972; Schechter *et al.*, 1973). We feel that the pmr results discussed below, particularly with regard to the interaction of His-119 with bound nucleotide, demonstrate that the pmr technique can be used in the light of X-ray crystallographic results to reveal subtle details of molecular interaction that neither technique can uncover when used separately.

Experimental Section

Materials. Ribonuclease A was purchased from Worthington Biochemical Corporation in the phosphate free lyophilized form, lot OLA, and was stored at −20° over anhydrous calcium sulfate.

Cytidine 2′,3′-cyclic phosphate, lot 40C-0200, and adenosine-5′-monophosphoric acid, lot 47B-7270, were purchased from Sigma Chemical Co. and were used without further purification. They were stored at 0–5° over P_2O_5.

Adenosine 5′-methyl phosphate was synthesized from 5′-AMP according to the method of Khorana and coworkers (Smith *et al.*, 1958) with the following exception. The ammonium salt of the monomethyl ester was dried under vacuum for 2 days over P_2O_5 at room temperature. Elemental analysis of this ammonium salt corresponded to the monohydrate. Later, the ammonium salt of the monomethyl ester was converted to the sodium salt *via* a Dowex 50 [Na^+] column. Descending paper chromatography with isopropyl alcohol–concentrated NH_4OH–water (7:1:2, v/v) showed no detectable 5′-AMP in the final product.

Concentrations were determined spectrophotometrically using the following extinction coefficients: ribonuclease A, 11,900 at 280 mμ (Meadows *et al.*, 1969); cyclic CMP, 8650 at 268 mμ (Wigler, 1968); 5′-AMP, 15,300 at 260 mμ (Dawson *et al.*, 1969); methyl 5′-AMP, 15,300 at 260 mμ (assumed to be the same as that of 5′-AMP).

Kinetic Methods. The following buffer systems were used in the kinetic determinations: formic acid–sodium formate, pH 4.11; acetic acid–sodium acetate, pH 4.58 and 5.07; malonic acid–sodium malonate, pH 5.57 and 6.10; imidazole–imidazolium chloride, pH 6.37, 6.93, and 7.40; Tris–Tris-HCl, pH 7.80 and 8.30. All buffers are 0.1 M and all were brought to an ionic strength of 0.2 M with sodium chloride.

Initial velocities of ribonuclease catalyzed cyclic CMP hydrolysis were measured according to the assay of Crook *et al.* (1960) using a Gilford Model 2000 absorbance recorder equipped with a Beckman DU monochromator, and a Neslab temperature regulated bath and circulator.

The reaction rate was followed by measuring the change in absorbance with time at wavelengths of 286, 292, and 294 mμ using rectangular quartz cells of 10, 2, and 1 mm path lengths. The monochromator was operated at a constant slit width of 0.40 mm. The change in extinction coefficient for cyclic CMP hydrolysis was measured, and the validity of Beer's law checked at each pH and wavelength used in the assays. All initial velocities were determined at 32 ± 0.5°. The reaction mixture without enzyme was equilibrated with a 32° water bath for at least 12 min before the reaction was initiated. Measurement or the optical density change started from 10 to 15 sec after addition of the enzyme.

Each initial velocity corresponding to a particular pH, substrate, and modifier concentration was determined in triplicate.

Nmr Methods. All spectra were recorded at 100 MHz with a Varian HA-100 spectrometer operated with an internal lock system and equipped with a Varian V-4315 digital readout frequency counter and a V-6040 variable temperature controller. The spectrometer was interfaced with a Varian C-1024 time averaging computer to improve the signal-to-noise ratio.

Spectra were collected in two ways. For most of the free enzyme spectra the system was operated in the conventional manner with the frequency sweep generated by the mechanically driven audiooscillator of the flat bed recorder. For all other spectra, an alternate means of sweeping the frequency devised by Dr. J. W. Faller (Yale University) was used to avoid excessive wear on the recorder assembly. Here, the frequency is swept using a Hewlett-Packard 3310A Function Generator which is driven by a ramp voltage from the C-1024 computer.

All samples were made up in 0.2 M NaCl in D_2O, and the pD was adjusted using solutions of DCl and NaOD in D_2O. The pD was measured using a Radiometer Model 4 pH meter equipped with a glass microelectrode, and was not corrected for isotope effects (Glascoe and Long, 1960). The pD of each sample was checked before and after each spectrum,

[1] The abbreviations are: AMP, adenosine monophosphate; CMP, cytidine monophosphate; UpA, (3′,5′)-uridyladenosine; UpcA, a phosphonate analog of Upa in which the 5′ oxygen of adenosine is substituted by a methylene group; MeAMP, methyl ester of AMP.

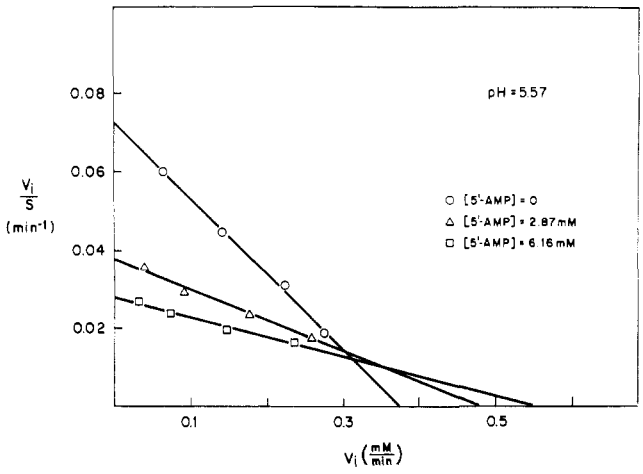

FIGURE 1: Eadie plots exhibiting the effects of 5'-AMP on the kinetics of ribonuclease A catalyzed hydrolysis of 2',3'-cyclic CMP at pH 5.57; each data point is an average of three separate initial velocity determinations.

and the spectrum was only accepted if the measurements agreed to within 0.02 pH unit.

Precision bore nmr tubes with coaxial inserts containing hexamethyldisiloxane were used. Hexamethyldisiloxane served as a reference and provided the lock signal. All chemical shifts are reported as cycles per second downfield from hexamethyldisiloxane. The probe temperature was maintained at 32°.

Since both C-2 and C-8 protons of the purine ring resonate in the same frequency region of the pmr spectrum as the C-2 proton of the imidazole ring, the C-8 proton was exchanged for deuterium in order to simplify the spectra of samples containing both enzyme and 5'-AMP or the methyl ester. The exchange was accomplished as follows: 500 mg of nucleotide in about 15 ml of D_2O was brought to pH 11.5–12.0 with NaOD, and refluxed for about 20 min; then the solution was reduced to a small volume under vacuum; this procedure was repeated once. 5'-AMP and the methyl ester were checked for hydrolytic decomposition after undergoing exchange by paper chromatography, and both were found to be stable to the exchange procedure.

Results

Kinetic Analysis of the Effects of 5'-AMP on Ribonuclease A Activity. Ribonuclease A catalyzed hydrolysis of cyclic CMP has been shown to follow simple Michaelis–Menten kinetics (Herries *et al.*, 1962). The initial velocity, v_i, is described by

$$v_i = \frac{-d[S]}{dt} = \frac{k_{cat,app}[E_0][S]}{K_{m,app} + [S]} \quad (1)$$

Of the several methods described in the literature for analyzing this type of kinetics, we have chosen the linear $v_i/[S]$ *vs.* v_i form (Eadie, 1942) for the present work both because the data points are weighted more evenly, and because the extent of enzyme saturation with substrate is directly observable with this method (Wilkinson, 1961).

Equation 1 may be rearranged to

$$\frac{v_i}{[S]} = \frac{v_i}{K_{m,app}} + \frac{V_{max,app}}{K_{m,app}} \quad (2)$$

where $V_{max,app} = k_{cat,app}[E_0]$.

Initial velocities were measured at various concentrations of cyclic CMP in the presence of constant 5'-AMP and enzyme concentrations. In the presence of 5'-AMP, ribonuclease obeys Michaelis–Menten kinetics. Eadie plots determined for three different 5'-AMP concentrations are shown in Figure 1.

In the presence of 5'-AMP, ribonuclease A displays mixed kinetics, *i.e.* both $K_{m,app}$ and $k_{cat,app}$ are raised. Since the effect is larger on $K_{m,app}$ than on $k_{cat,app}$, at low unsaturating substrate concentrations the enzyme activity is inhibited, and at high saturating substrate concentrations the enzyme is activated by 5'-AMP. Such behavior appears to be invariant with pH as we have also observed this same type of mixed kinetics at pH 4.11 and 6.93.

Activation of an enzyme requires the existence of the ternary complex ESM where M is the modifier, in this case 5'-AMP. ESM necessarily converts to product faster than the ES complex.

The simplest explanation for the raise in $K_{m,app}$ is a competitive equilibrium, $E + M \rightleftharpoons EM$, for which EM has a lower affinity for the substrate than does free enzyme.

Considering all complexes to be in equilibrium with each other

$$\begin{array}{ccccc} E & \overset{+S}{\rightleftharpoons} & ES & \xrightarrow{k_{cat}} & E + P \\ \Updownarrow{\scriptstyle +M} & & \Updownarrow{\scriptstyle +M} & & \\ EM & \overset{+S}{\rightleftharpoons} & ESM & \xrightarrow{k_{cat}'} & E + P + M \end{array}$$

where $k_{cat}' > k_{cat}$.

Assuming all binding equilibria to be rapid relative to k_{cat} and k_{cat}', $K_m = K_s = [E][S]/[ES]$, $K = [EM]/[E][M]$, $K' = [ESM]/[ES][M]$, and (Laidler, 1958)

$$v_i = \frac{(k_{cat} + k_{cat}'K'[M])[E_0][S]/K_m}{1 + [S]/K_m + K[M] + K'/K_m[S][M]} \quad (3)$$

The equilibrium assumption is valid for substrate binding since temperature jump kinetic studies (Erman and Hammes, 1966) have demonstrated that the Michaelis constant, K_m, is a true equilibrium constant for cyclic CMP at pH 6.0. As will be shown below, k_{cat}'/k_{cat} is small and so does not affect the equilibrium assumption for substrate binding. The relaxation times governing 5'-AMP binding, however, have not been measured. The equilibrium for 3'-pyrimidine nucleotide binding is also rapid compared to k_{cat} (Hammes and Walz, 1969).

Equation 3 can be arranged to the Eadie form

$$\frac{v_i}{[S]} = \frac{-1}{K_m}\left(\frac{1 + K'[M]}{1 + K[M]}\right)v_i + \frac{[E_0](k_{cat} + k_{cat}'K'[M])}{K_m(1 + K[M])} \quad (4)$$

where the slope $m = -1/K_{m,app} = (-1/K_m)[(1 + K'[M])/(1 + K[M])]$. Further

$$m/m_0 = \frac{1 + K'[M]}{1 + K[M]} \quad (5)$$

where $m_0 = -1/K_m$ is the slope of the Eadie plot at [5'-AMP] = 0.

Solving eq 5 using the slopes and corresponding 5'-AMP concentrations from Figure 1, we find $K = 0.64\ mM^{-1}$, $1/K = 1.55$ mM, $K' = 0.047\ mM^{-1}$, and $1/K' = 20.8$ mM.

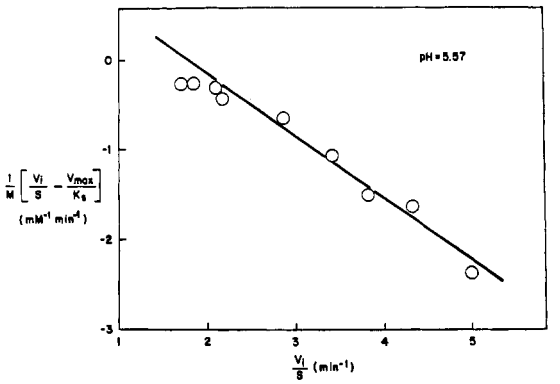

FIGURE 2: Determination of the binding constant for 5'-AMP at pH 5.57. The analysis is based on eq 8 in the text. Each data point corresponds to a different 5'-AMP concentration and is an average of three separate initial velocity determinations.

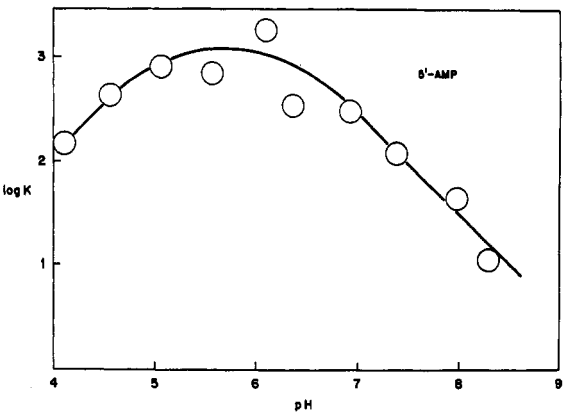

FIGURE 3: The pH dependence of the binding constant for 5'-AMP. Each K determination was based on the analysis of eq 8 in the text. A minimum of 15 initial velocities was measured to determine K at each pH.

From eq 4

$$\text{intercept} = \frac{V_{max,app}}{K_{m,app}} = \frac{[E_0](k_{cat} + k_{cat}'K'[M])}{K_m[1 + K[M]]} \quad (6)$$

Solving for k_{cat} and k_{cat}' using the intercepts from Figure 1 and the above values of K and K' we find $k_{cat} = 3.08$ sec^{-1} and $k_{cat}' = 10.2$ sec^{-1}.

For this type of mixed kinetics it is worth noting that a minimum of three Eadie plots corresponding to three different 5'-AMP concentrations are required to calculate all five independent kinetic parameters.

pH Profile of the Binding Constant for 5'-AMP. The binding constant, K, for 5'-AMP was determined at each pH by measuring v_i at various concentrations of 5'-AMP at constant cyclic CMP concentration. To calculate K from such data, it is necessary that the condition $[S] \ll K_m$ be met at each pH. The pH region in which it is most difficult to reach this condition is 5–6 where the minimum occurs in the bell-shaped pH profile of K_m at 25° (Herries *et al.*, 1962). At pH 5.57 and 32°, K_m is 2.53 mM; since a [S] of 0.156 mM was used, $[S]/K_m = 0.06$. Assuming the pH of minimum K_m does not change with a 7° rise in temperature, the condition $[S] \ll K_m$ prevailed at all pH values of the K profile.

Again, considering eq 3, we have $1 \gg [S]/K_m$. From the Eadie plots, we know $K > K'$; hence, $K[M] \gg K'[S][M]/K_m$ and eq 3 reduces to

$$v_i = \frac{(k_{cat} + k_{cat}'K'[M])[E_0][S]/K_m}{1 + K[M]} \quad (7)$$

$$v_i + v_iK[M] = \frac{k_{cat}[E_0][S]}{K_m} + \frac{k_{cat}'K'[M][E_0][S]}{K_m}$$

for $[S] \ll K_m$ and [5'-AMP] = 0, $v_{i_0} \equiv k_{cat}[E_0][S]/K_m$ and

$$\frac{v_i}{[M]} + v_iK = \frac{k_{cat}'K'[E_0][S]}{K_m} + \frac{v_{i_0}}{[M]}$$

$$\frac{v_i - v_{i_0}}{[M]} = (-K)v_i + \frac{k_{cat}'K'[E_0][S]}{K_m} \quad (8)$$

Plotting $(v_i - v_{i_0})/[M]$ *vs.* v_i, or $(1/[M])\{v_i/[S] - (V_{max}/K_m)\}$ *vs.* $v_i/[S]$ when two different substrate concentrations are used at the same pH, should fix the data on a straight line with slope $-K$. The results of this kind of plot at 5.57 are shown in Figure 2. In general, data points tended to spread at high v_i values because $v_i - v_0$ values are smaller, 1/[M] becomes larger, and hence the error is magnified at high v_i.

Initial velocities were measured in triplicate for at least five different 5'-AMP concentrations in every K determination. The pH profile of log K is shown in Figure 3.

Pmr Titration of the Histidine Residues of Ribonuclease A. Resolution of the C-2 proton resonance lines for all four histidine residues of ribonuclease A was first reported by Jardetsky and coworkers (Meadows *et al.*, 1967) operating at 100 MHz. By measuring the change in the chemical shift of each C-2 proton line as the pH is varied from values of 3–9, titration curves for the individual histidine residues have now been determined by several different groups of researchers.

Ruterjans and Witzel (1969), King and Bradbury (1971), and Cohen and coworkers (1970) all have observed irregularities in the shapes of the His-12 and His-119 titration curves in the form of skews near the titration midpoint (pD ~6). In contrast, Jardetsky and coworkers (Meadows *et al.*, 1969) have reported that they have found no evidence of such skewing.

These same titration curves determined in our laboratory are shown in Figure 4. The assignments indicated are those of Meadows *et al.* (1968). In agreement with previously reported findings, the resonance line assigned to His-48 broadens greatly as the pD is raised, and finally disappears above pD 5.9 in the chloride salt system.

Skewing in the His-12 and -119 titrations is not observable in Figure 4. However, we have found other irregularities in the titrations of His-12 and His-119. The titration to low pD was not completely reversible. Samples which were brought to a pD of 3 and then titrated back to pD 5.90 exhibited His-12 and His-119 chemical shifts which were some 7 and 13 Hz, respectively, further downfield than the corresponding shifts of samples at pD 5.90 which had not been previously exposed to low pD conditions. The titration of His-105 appeared to be completely reversible under these conditions. Furthermore, the His-12 and -119 titration curves, although they may appear quite normal to the eye, do not have a shape predicted by a sample acid dissociation process (see below). These results prompted us to examine these data in more detail.

The observed chemical shift for a simple acid such as

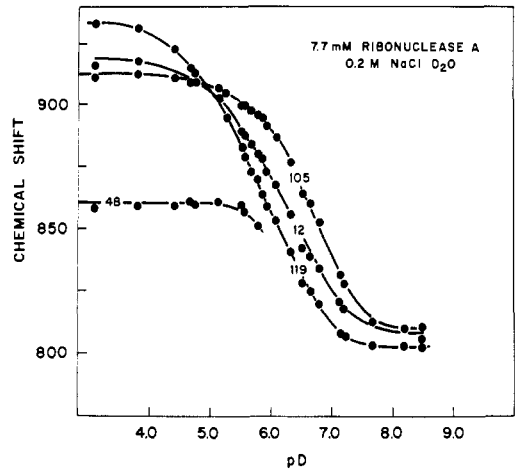

FIGURE 4: Titration curves for the individual histidine residues of ribonuclease A. Chemical shift indicates the resonance line positions of imidazole C-2 proton measured downfield from the hexamethyldisiloxane standard. The assignments indicated are those originally proposed by Meadows *et al.* (1968).

imidazolium ion for which the acid dissociation equilibrium is rapid on the nmr time scale is an average

$$\delta = \delta_{Im}\frac{[Im]}{[Im] + [ImH^+]} + \delta_{ImH^+}\frac{[ImH^+]}{[Im] + [ImH^+]} \quad (9)$$

where δ_{Im} and δ_{ImH^+} are the chemical shifts of imidazole, Im, and imidazolium ion, ImH^+, respectively. For the acid dissociation

$$K_a = \frac{[H^+][Im]}{[ImH^+]}$$

$$\frac{[Im]}{[Im] + [ImH^+]} = \frac{K_a}{K_a + [H^+]} \quad (10)$$

and

$$\frac{[ImH^+]}{[Im] + [ImH^+]} = \frac{[H^+]}{K_a + [H^+]} \quad (11)$$

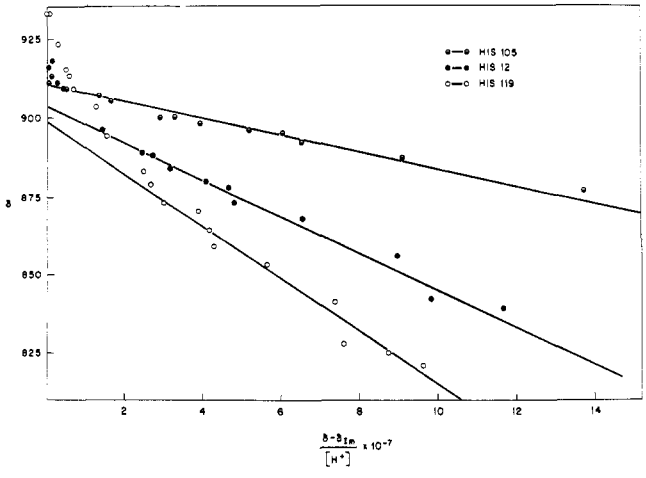

FIGURE 5: Titration data of three of the four histidine residues plotted according to eq 12.

TABLE I: Line Widths of the Histidine C-2 Proton Resonance Lines in Hertz.[a]

pD	His-12	His-119	His-105
6.78	4.7	6.7	5.7
6.63	5.2	7.8	6.7
6.50	6.2	8.3	8.3
5.89	5.2	7.3	5.7
5.84	6.2	6.8	6.2
5.64	5.7	7.8	6.2
3.78	$\leq$7.3	8.3	$\leq$8.3
3.14	$\leq$5.2	7.3	$\leq$6.2
3.15	$\leq$4.7	7.3	$\leq$6.2

[a] The estimated error is $\pm$1 Hz. The assignments are those indicated by the smooth curves in Figure 5. The line widths were most easily measured in the pH range 5.5–6.8 where the three resonance lines are well separated. At pH values below 4, the line farthest downfield is well separated from the other two partially overlapping lines. When two lines partially overlapped, only the upper part bound to the half-width could be measured.

Substitution of eq 10 and 11 into eq 9 gives

$$\delta = \delta_{Im}\left(\frac{K_a}{K_a + [H^+]}\right) + \delta_{ImH^+}\left(\frac{[H^+]}{[H^+] + K_a}\right)$$

or

$$\delta = -K_a\left(\frac{\delta - \delta_{Im}}{[H^+]}\right) + \delta_{ImH^+} \quad (12)$$

Plots of δ *vs.* $(\delta - \delta_{Im})/[H^+]$ for each histidine residue are shown in Figure 5. The His-105 plot is linear in accordance with simple acid titration behavior. The His-119 data, however, deviate from a straight line in the region of the plot corresponding to low pD. The His-12 plot also breaks from a straight line at low pD but to a lesser extent than His-119. These deviations from linearity both occur in the same pD region where the titration curves assigned to His-12 and His-119 intersect (pD $\sim$5.2 in Figure 4). The question then arises concerning the true continuity in the His-12 and His-119 titration curves through the point at which they intersect. In fact, the whole question of assignment of these two titration curves is involved here because the assignment of His-119 in ribonuclease A (Meadows *et al.*, 1968) is based on its abnormally high chemical-shift value at low pD in both ribonuclease A and ribonuclease S (see Discussion).

To resolve this question, the assignments of the His-12 and -119 curves indicated in Figure 4 on the low pD side of their intersection point were switched and the data again replotted according to eq 11. The new plots were no more linear than before and hence were of no help in choosing the correct continuities.

The line widths of the three histidine resonance lines were examined on both the low and high pD sides of the intersection in the titration curves. The results shown in Table I indicate that the resonance lines assigned originally to His-119 are broader than those of His-12 and -105 on both sides of

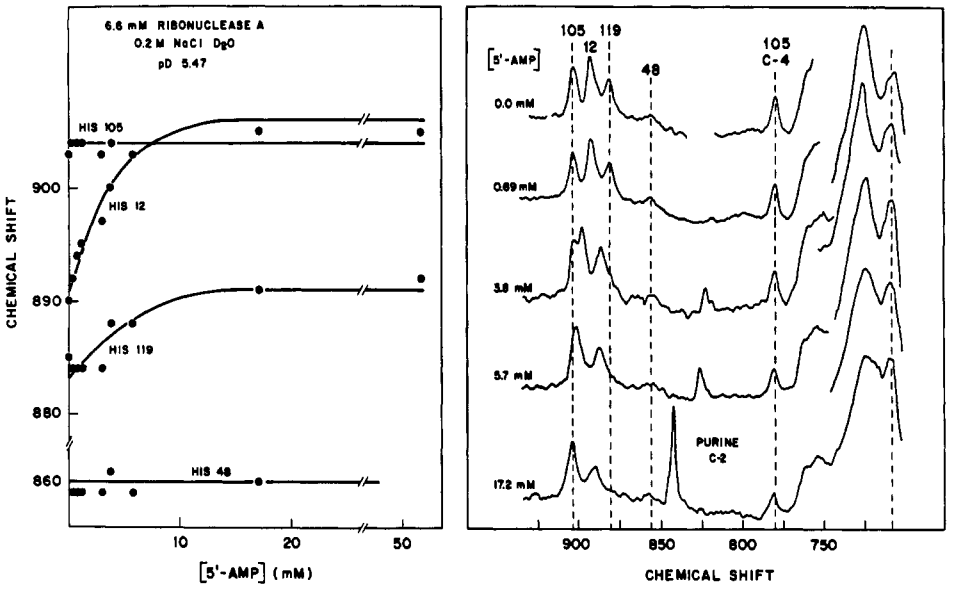

FIGURE 6: Right, the effects of increasing 5'-AMP concentration on the ribonuclease A pmr spectrum. The large aromatic envelope is in the 650–750-Hz region while the imidazole C-2 proton lines occur in the 850–950-Hz region. Left, the dependence of the imidazole C-2 proton chemical shift on 5'-AMP concentration at pH 5.47 for each histidine residue. At 5'-AMP concentrations greater than 17 mM, the His-48 line is obscured by the large 5'-AMP purine C-2 proton envelope.

the point of intersection in the titration curves. Further, the lines assigned to His-119 have the same width within experimental error throughout the pD range investigated. Thus, the continuity in the differences in line width among the three histidine residues correlates with the continuities in the titration curves which were originally drawn by visual inspection. This correlation, in turn, substantiates the assignments of the His-12 and His-119 resonances as originally proposed (see Discussion).

Departure from simple acid titration behavior has also been observed by Cohen and coworkers (1973) for His-12 and -119. These workers have collected over 50 data points for each titration curve at 220 MHz and have used various models for interaction between the imidazole moiety and neighboring titratable groups to computer curve fit the histidine titration curves directly. They have also found asymmetry in the acid pD region of the curve which has been designated His-119. These His-119 data could be fit accurately with a pK_a of 6.1 for His-119 imidazolium and a model incorporating a neighboring interacting group with a pK_a of 4.6. For the His-12 titration they have observed small asymmetries in both the acid and alkaline pD regions. The data could be fit with a pK_a of about 6.2 for His-12 imidazolium and pK_a values of 5 and 8.4 for two neighboring interacting, titratable groups. In agreement with our results, they found that these asymmetries were not observable as skews but become obvious only after comparison with a simple titration curve.

Titration of Ribonuclease A with 5'-AMP at Constant pD. The effects on the ribonuclease pmr spectrum of increasing the 5'-AMP concentration at constant enzyme concentration and pD are shown in Figures 6 and 7. At both pD 5.47 and 7.00, the C-2 proton resonances of His-12 and -119 are selectively shifted downfield with increasing apparent 5'-AMP concentration. The effect is larger on His-12, a total shift of 14 and 55 Hz being observed upon saturation with 5'-AMP compared to approximately 7 and 5 Hz for His-119 at pD 5.47 and 7.00, respectively. There is no observable effect on the His-105 resonances nor on the greatly broadened His-48 peak at pD 5.47.

These results with 5'-AMP contrast dramatically with those found by Jardetsky and coworkers (Meadows and Jardetsky, 1969; Meadows *et al.*, 1969) and Ruterjans and Witzel (1969) for the binding of the isomeric cytidine monophosphates. For both 2'- and 3'-CMP, the His-119 resonance is perturbed upfield to a much greater extent than that of His-12. The His-48 resonance also shifts upfield while the His-105 resonance is unaffected by CMP binding. Jardetsky's group has also observed a shielding effect due to CMP binding on a peak under the large aromatic envelope with an area corresponding to approximately five protons. This large peak shifts upfield and broadens greatly upon binding of all the

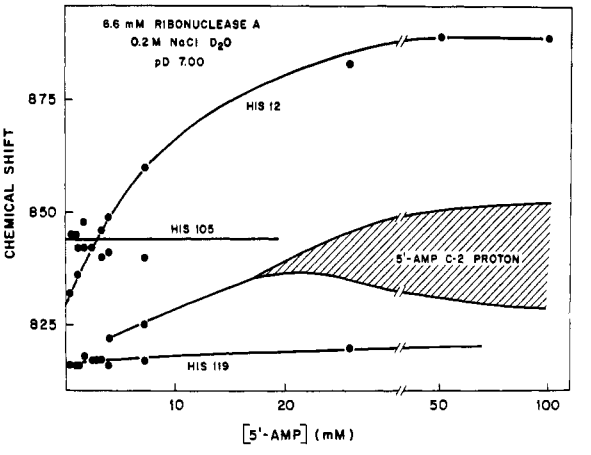

FIGURE 7: The dependence of the imidazole C-2 proton line position on the concentration of 5'-AMP at pH 7.00 for each histidine residue. At very high 5'-AMP concentrations, the His-105 and His-119 lines are obscured by the large 5'-AMP purine C-2 proton envelope.

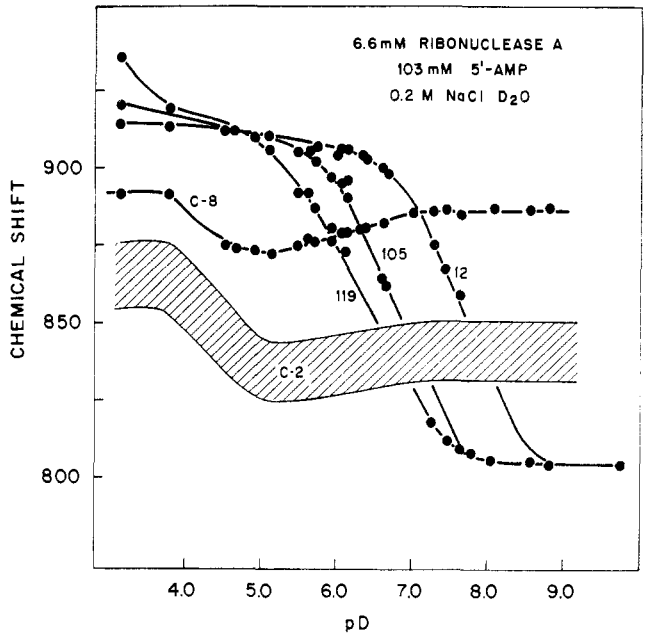

FIGURE 8: Titration curves of the individual histidine residues of ribonuclease A measured in the presence of a constant excess concentration of 5'-AMP. The residual 5'-AMP purine C-8 proton line is due to incomplete total exchange of this C-8 proton for deuteron. The pH dependence of the purine C-2 and C-8 proton chemical shifts reflects the titration of both the adenine ring and the phosphate moiety of unbound 5'-AMP.

isomeric cytidine mononucleotides and cytidine as well (Meadows *et al.*, 1969). The peak is not influenced to any observable extent by phosphate, sulfate (Meadows *et al.*, 1969), or 5'-AMP as observation of Figure 6 indicates.

Titration of the Histidine Residues of Ribonuclease A in the Presence of Excess 5'-AMP. To help interpret the results of Figures 6 and 7, the histidine residues were titrated in the presence of a constant excess concentration of 5'-AMP (Figure 8). The apparent 5'-AMP concentration of 103 mM is sufficient to saturate the enzyme at both pD 5.47 and 7.00.

The spectra represented in Figure 8 were complicated by the presence of a small C-8 proton peak due to incomplete total exchange of the purine C-8 proton for deuterium, and a huge purine C-2 proton peak due to the large excess of 5'-AMP. Unfortunately, the positions of these purine peaks are in the region of the pmr spectrum through which the histidine C-2 proton peaks move during the titration. Nevertheless, we were able to collect sufficient data to reconstruct the titration curves and determine the corresponding K_a values assuming a simple acid dissociation for each curve (see Table II).

TABLE II: Effect of 5'-AMP on the pK_a of Each Histidine Residue of Ribonuclease A.

Residue	Free Enzyme	Enzyme + 5'-AMP
His-105	6.58	6.58
His-12	6.21	7.6
His-119	6.06	6.3

The titration curve for His-105 in Figure 8 is superimposable on that of ribonuclease alone. On the other hand, the pK_a of His-12 is perturbed from 6.2 to 7.6 and that of His-119 from 6.05 to 6.3 upon addition of 5'-AMP. Since the enzyme is still saturated with 5'-AMP at pD 7, the pK_a of 6.3 for His-119 is that for the actual enzyme–5'-AMP complex. The fully protonated His-119 peak is also shifted some 20 Hz (0.2 ppm) upfield in the pH 4.5–5.0 region of the curve where the enzyme is still saturated with 5'-AMP. This shielding effect on His-119 is in opposite direction to those seen in the presence of the isomeric CMPs. Meadows *et al.* (1969) report deshielding effects of 25–20 Hz at low pD in the presence of 2'- and 3'-CMP, respectively.

These titration techniques, used originally by Meadows and Jardetsky with 3'-CMP, are complementary. Titration with nucleotide at constant pD is necessary to identify the correct assignments in Figure 8. On the other hand, titration of enzyme plus excess nucleotide is necessary to unscramble the effects observed in Figures 6 and 7 in terms of effects on pK_a values and specific magnetic effects on δ_{ImH^+}.

Effects of 5'-AMP Self-Association on the Results. Ts'o and coworkers (1963) by nmr and Van Holde and Rossetti (1967) by equilibrium sedimentation have demonstrated that 5'-AMP aggregates in water to form most likely linear stacks of monomer. It is necessary to determine what effect these stacking equilibria might have on our calculations on the binding of 5'-AMP to ribonuclease A.

Since there is no quantitative data available in the literature on the extent of 5'-AMP stacking, we have determined the extent of purine stacking in solution for which quantitative data are available, and will assume that 5'-AMP stacking is less favorable than purine stacking. This assumption is reasonable since in the pH region investigated (pH 4–8.3) 5'-AMP is charged while purine is not.

We have calculated the concentration of purine monomer in grams/milliliter at various concentrations of total purine (grams/milliliter) using the indefinite stacking model (Ts'o *et al.*, 1963) and a value of 23 ml/g (Van Holde and Rossetti, 1967) for the equilibrium constant governing the addition of each monomer to the polymeric stack. The monomer and total purine concentrations in grams/milliliter were converted to the real and apparent molar concentrations, respectively, by dividing each by 120 g/mol, the molecular weight of purine.

The discrepancy between these real and apparent monomer concentrations becomes significant (>5%) only at concentrations of 0.01 M and above for purine. For 5'-AMP, this discrepancy will only become significant at still higher concentrations. For the calculations of k'_{max}, K, and K' at pH 5.57, the highest concentration of 5'-AMP was 0.0061 M. The effect of 5'-AMP stacking, therefore, will be negligible here.

For the pH profile of log K, concentrations of up to 50 mM 5'-AMP were used where self-association may no longer be safely neglected. However, since the real [M] is not a linear function of apparent [M], the self-association will not simply change the slope of the $(v_i - v_{i_0})/[M]$ *vs.* v_i plots. Rather, the self-association should manifest itself as a deviation from linearity in the high [M] region or low v_i/S region of the plot. A slight deviation in the direction expected for the self-association may be seen in Figure 2 and was observed at several different pH values. If the slopes are taken then at the linear regions of these plots, the self-association may safely be neglected in the K calculations.

Studies on the Binding of 5'-AMP Methyl Ester (Me-5'-AMP) to Ribonuclease A. The effect of methyl 5'-AMP on the kinetics of cyclic CMP hydrolysis was determined at pH 6.93.

The results are as follows

[c-CMP] (mM)	[Me-5′-A MP] (mM)	$(v_i)_{Me\text{-}5'\text{-}AMP}/v_i$
0.83	41.8	0.75
20.9	60.1	1.20

The effect of Me-5′-AMP is of the same nature as that of 5′-AMP. The hydrolysis is inhibited and activated at unsaturating and saturating substrate concentrations, respectively. Both $K_{m,app}$ and $V_{max,app}$ are increased in the presence of the methyl ester; the effect is larger on $K_{m,app}$. The very small effects of large concentrations of Me-5′-AMP on the initial velocity unfortunately prohibit the kind of quantitative analysis performed in the 5′-AMP case.

Consistent with these kinetic results is our observation that the presence of Me-5′-AMP has no effect on the histidine resonances at pH 7.00 up to an apparent concentration of 40 mM. At higher Me-5′-AMP concentrations, the results are obscured by the presence of the large purine C-2 proton resonance envelope. This weak 5′-AMP binding probably reflects both the small affinity of the enzyme for monoanionic phosphates and a strong tendency for the methyl ester to self-associate.

Discussion

Pmr Titration of Ribonuclease A. The assignment of the His-12 and His-119 titration curves depends critically on the concatenations in these curves in the low pD region. The original assignments in ribonuclease A (Meadows *et al.*, 1968) were made by determining the correct assignments in the modified derivative, ribonuclease S, and extending these to A presumably by comparing the K_a values and the shapes of each titration curve in both enzymes. Extension based on pK_a comparisons has been criticized by King and Bradbury (1971) for the pK_a values of both His-12 and His-119 change in the modification of ribonuclease A to S. The extension based on differences in the shapes of the two curves in both enzymes is feasible since the work of Schechter *et al.* (1973) and the results of Figure 5 show that the shapes of the two curves are quite different at low pD. As we have already mentioned, however, there is ambiguity with regard to assigning the correct continuities, *i.e.*, the correct abnormal shapes in the low pD region. Because the shapes of both the His-12 and His-119 curves are irregular in this region of intersection, there is no reason to assume that the continuities which are perhaps visually obvious are the true continuities.

Examination of the line-width data of Table I indicates that the continuity in the differences in line width between the His-12 and -119 lines correlates with and hence supports the "visually obvious" concatenations originally proposed for these titration curves of ribonuclease A. If the "visually obvious" continuities in the ribonuclease S titration are also correct, then the curve which raises to the highest chemical-shift value in both enzymes at low pD is most probably that of His-119 in both ribonuclease A and S.

The abnormal behavior observed in Figure 5 demonstrates that there is a change in the environment of His-12 and His-119 which accompanies titration to low pD. The shifts in the His-12 and His-119 resonances much farther downfield than is predicted by eq 11 may be explained by two different mechanisms. The pD-dependent change in the environment of each histidine may strengthen the acidity of each histidine, or alter the magnetic environment of each imidazolium C-2 proton; both mechanisms could be operative. It is unlikely that large pH-dependent conformational changes are occurring in the enzyme tertiary structure, in view of the quite normal titration observed for His-105, and the lack of evidence for any gross conformational effect at pH 5 for this very extensively studied enzyme.

The X-ray crystallographic results on the structure of ribonuclease S suggest that His-119 can take up any of four different positions at the active site in the crystal (see introductory statement). The biphasic curve in Figure 5 is quite consistent with such a picture, and suggests that different His-119 positions are stabilized by different conditions of pH.

The effects on His-12 and His-119 at low pH may very likely involve a His-119–Asp-121 interaction as the crystallographic model of ribonuclease S (Richards and Wyckoff, 1971) and curve-fitting the His-119 titration curve (Schechter *et al.*, 1973) suggest. When Asp-121 becomes protonated at low pH, its interaction with His-119 in position IV would be destroyed, and the relative population of His-119 shifts to positions II and III. His-119 in position II is very close to His-12; the distance of the His-119 C-2 to the nearest N of His-12 is approximately 6 Å in the crystallographic model. An unfavorable imidazolium–imidazolium charge interaction could occur which would effectively lower the pK_a of both residues.

Binding Site of 5′-AMP. In the three-dimensional model of the ribonuclease S–3′-CMP complex (Richards and Wyckoff, 1971) Phe-120 lies adjacent to the cytosine ring in the nucleoside binding pocket (B_1). This strongly suggests that the large five-proton aromatic peak which Jardetsky's group (Meadows *et al.*, 1969) found to shift upfield upon binding of all the isomeric cytidine mononucleotides be assigned to Phe-120, and that perturbation of this peak is intimately associated with binding in the B_1 site at the enzyme surface.

That 5′-AMP has no observable effect on the aromatic peak associated with Phe-120 indicates that 5′-AMP is not bound to the enzyme in the pyrimidine (B_1) binding site. Yet the effects of 5′-AMP on His-12 and -119 resonances discussed below strongly suggest that the phosphate of 5′-AMP is bound near or at these two residues, and hence in a position similar to the phosphates of bound cytidine mononucleotides. All this, of course, substantiates previous X-ray crystallographic results (Richards and Wyckoff, 1971).

Careful comparison of Figures 4 and 8 at pD 5 reveals that 5′-AMP binding causes a selective upfield shift in the fully protonated His-119 resonance of about 0.2 ppm relative to that of ribonuclease A. The effect is in opposite direction to that observed with 2′- or 3′-CMP, both of which cause downfield shifts. Hence this effect cannot be associated with phosphate binding alone but must be related to the nature of the binding sites for the nucleoside bases.

Some suggestions may be made about the origin of this selective upfield shift in the His-119 resonance in light of the X-ray crystallographic results available on 5′-AMP binding (Richards and Wyckoff, 1971). An upfield shift is quite consistent with a base stacking interaction between the adenine base of the 5′-AMP and His-119. A similar upfield shift of 0.2 ppm has been found in comparing the C-8 proton of adenine in 3′-AMP to that in ApA (the "dimerization shift") (Schweizer *et al.*, 1968). This system is quite analogous to the proposed adenine–histidine interaction since the C-8 proton of adenine is a C-2 imidazole-like proton, and ApA is known to assume a base-stacked conformation in solution (Schweizer *et al.*, 1968).

Another quite plausible explanation for the upfield shift, suggested by the X-ray results, is that 5′-AMP binding stabilizes a salt bridge interaction between His-119 in position IV and the carboxyl of Asp-121. Bound 5′-AMP either surrounds the salt bridge with a less polar microenvironment or positions His-119 properly for maximum interaction with Asp-121, or both. The salt bridge interaction would increase the diamagnetic shielding at the C-2 proton (upfield shift) by removing positive charge from the imidazolium ring of His-119.

Purine nucleotide binding to ribonuclease has been demonstrated by a variety of other types of physical studies (Hummel *et al.*, 1961; Barnard and Ramel, 1962; Myer and Schellman, 1962; Deavin *et al.*, 1968; Anderson *et al.*, 1968).

Interpretation of pH Profile of 5′-AMP Binding. The question of primary importance concerning the binding profile is which groups of the free enzyme and nucleotide are responsible for the low and high pH arms of the profile. The slopes of +1 and −1, respectively, suggest that only one titratable group is responsible for each arm.

The low pH arm of nucleotide binding profiles has been explained by Jardetsky's group (Meadows *et al.*, 1969) as due to titration of the nucleotidic phosphate assuming the dianionic form of the nucleotide to predominate the binding, and by Hammes and coworkers (Anderson *et al.*, 1968) as titration of an enzyme acid group assuming monoanionic nucleotide to predominate the binding to enzyme. The distinction here between the two proposed binding mechanisms is artificial since both result in the same enzyme–nucleotide complex. That the methyl ester of 5′-AMP binds only very weakly to the enzyme suggests that at least in the 5′-AMP case, the dianionic phosphate form of the nucleotide is the predominant binding form. Weak binding of 5′-MeAMP which is due to steric hindrance of the 5′-methyl group is not likely since there is space at the active site for substrate 3′-pyrimidine nucleoside esters of 5′-AMP. The simplest explanation, then, is that the left arm of the binding profile is controlled by titration of an acid group of the free enzyme. The pmr titration (Figure 8) would strongly suggest that this acid is His-12.

There is evidence, however, that the true picture behind the nucleotide pH profile may be much more complicated than a simple interaction between a dianionic phosphate and protonated His-12. Firstly, the pH profile of 3′-CMP binding has the same shape as that of 5′-AMP, yet 3′-CMP binding has an apparently strong acid stabilizing influence on both His-119 and His-12 (Meadows and Jardetsky, 1969). Secondly, the T-jump work of Hammes' group on the 3′-pyrimidine nucleotides indicates that several pH-dependent processes are occurring in the binding process. In fact, the pH profile for the equilibrium constant governing the bimolecular relaxation process associated with 3′-UMP binding was found not to have the same shape as the binding constant profile (Hammes and Walz, 1969), The pH binding profiles, then, for the pyrimidine nucleotides seem to have a deceptively simple shape, and are a caution against placing too much faith in the interpretation of the 5′-AMP binding profile without additional T-jump kinetic data.

Knowledge of the pH profile of 5′-AMP binding is required for the correct interpretation of the titration curves of the histidine residues in the presence of an excess of 5′-AMP (Figure 8). Calculation of the degree of saturation of the enzyme with 103 mM 5′-AMP throughout the entire pH range is impossible without quantitative information on the extent of self-aggregation of 5′-AMP. It is apparent, however, from the shape of the binding profile, the extent of saturation indicated at pH 5.5 and 7.0 in Figures 6 and 7, and the known lack of dependence of 5′-AMP stacking on pH (Schweizer *et al.*, 1968) that the enzyme is not saturated at pH values much below 4 and above pH 7 in Figure 8. The enzyme is no longer saturated in the pH region at which titration of His-12 occurs. Hence, the pK_a of 7.6 measured for His-12 is an apparent pK_a which should be dependent on the concentration of 5′-AMP present, as is the case with CMP. The shape of the binding profile also provides an explanation for the downfield shift in the His-119 resonance at very low pD in Figure 8. If it is assumed that the binding profile does not change in shape down to pH 3, then this downfield shift at very low pH is due to the drop-off in the extent of saturation of the enzyme in this pH region. The chemical shift of His-119 changes from 918 Hz at 5.5 where the enzyme is completely saturated to 935 Hz at pH 3.15 where the enzyme is completely unsaturated with 5′-AMP.

Phosphate–Histidine Interaction in Nucleotide Binding and Its Implications for the Mechanism of Catalysis. The pH profile for 5′-AMP binding (Figure 3) is quite similar in shape to that for 3′-pyrimidine nucleotides and phosphate binding (Anderson *et al.*, 1968). The low and high pH arms of all four profiles have slopes of +1 and −1, and the pH maxima are all between 5.5 and 6. The comparison indicates that the shape of the binding profile is determined primarily by interaction of the phosphate of each nucleotide with the enzyme. This, in turn, suggests that although the base binding site is different for each, the phosphate binding site is similar for both 5′-AMP and 3′-CMP.

The relevance of inhibitor binding studies to the problem of how active-site amino acid residues are interacting with bound substrate may seem questionable when the studies center on titrations of these residues, and the inhibitor and substrate have different states of ionization above pH 6.

The model system studies of Westheimer and associates (Westheimer, 1968) of cyclic ethylene phosphate hydrolysis, however, suggest the existence of a pentacoordinate intermediate in ribonuclease catalysis. Such a species would be dianionic like the mononucleotide inhibitors, and it is to the nature of the enzyme–pentacoordinate intermediate interaction that our studies may apply.

Pmr titrations have shown that the binding of each of 2′-CMP, 3′-CMP, 5′-CMP (Meadows *et al.*, 1969), and now 5′-AMP has a strong acid stabilizing influence on His-12. That the effect is due solely to the presence of the negatively charged phosphate suggests salt bridge formation between His-12 imidazolium cation and the phosphate accompanies the binding of each nucleotide. In view of the differences in position of phosphate substitution for these nucleotides, especially in the isomeric CMP's, the enzyme nucleotide complex must have a certain flexibility to achieve a maximum interaction between His-12 and the phosphate. Such a flexibility has important implications for the mechanism of catalysis since the phosphate of bound substrate may very likely move about 2 Å in the formation of the pentacoordinate intermediate (Richards and Wyckoff, 1971). The His-12 imidazole may be quite capable of salt bridging with and hence stabilizing the pentacoordinate intermediate after abstracting a proton from the ribose C-2′-hydroxyl in step I (transesterification) catalysis.

In contrast to the 3′-CMP case, binding of 5′-AMP has a much smaller effect on the acidity of His-119. In fact, the pK_a of 6.3 is that of the actual ribonuclease 5′-AMP complex. A protonated His-119 is not required for 5′-AMP binding to occur. The relatively small effect on the pK_a suggests there is no strong salt bridge between the two. Other acid stabilizing

effects such as interaction with the carboxyl of Asp-121 could easily explain the small pK_a shift. Alternatively, there could be a strong salt bridge interaction between His-119 and the phosphate which is compensated for by an energetically unfavorable interaction between the adenine base and the His-119 imidazolium. The most important point to be made here is that the phosphate of bound 5′-AMP is at the phosphate binding site for 3′-CMP, yet the enzyme somehow is preventing a strong acid stabilization of His-119 imidazolium by the phosphate. This is perfectly consistent with the likely role of His-119 as a general acid catalyst protonating the adenosine cleaving group in the transesterification of CpA. In fact, it is most essential for the enzyme to temper a strong acid stabilization of His-119 by bound phosphate since such an interaction would severely limit His-119's effectiveness as a general acid catalyst at pH 7. Further, since the pK_a of His-119 is perturbed to only a relatively small extent, it follows that His-119 can play only a relatively small role in stabilizing the dianionic pentacoordinate intermediate in step I catalysis.

Finally, we note that the study of 5′-AMP binding would seem to have particular application to the mechanism of catalysis, for X-ray crystallographic results have strongly suggested (Richards and Wyckoff, 1971) that the active site has a catalytically active geometry with regard to His-119 when 5′-AMP is bound. In contrast, with CMP bound, His-119 assumes position III in the crystal, an orientation known to be abortive in transesterification and possibly abortive in hydrolysis as well.

Modification by 5′-AMP of the Rate of Cyclic CMP Hydrolysis. It has been demonstrated that the phosphate moieties of both 5′-AMP and 3′-CMP bind at or near the same site on the surface of the enzyme while the binding site for the base of each nucleotide is different. This clearly suggests that the inhibition by 5′-AMP of cyclic CMP hydrolysis is due to a binding competition between the nucleotides for this phosphate site. Although the phosphate binding site for cyclic CMP may be displaced some 2 Å from that of 3′-CMP and 5′-AMP (Richards and Wyckoff, 1971), such a displacement would be insufficient to remove spatial overlap between two such phosphate sites. Even if the binding of the two different phosphates were not mutually exclusive sterically, there still would be competition for interaction with the amino acid residues comprising the phosphate site, namely His-12 and perhaps His-119.

Activation by 5′-AMP of cyclic CMP hydrolysis under saturating conditions results in a factor of 3 in k_{cat} at pH 5.57. It is most reasonable that for activation to occur, the phosphate of 5′-AMP must be displaced from its inhibitory binding site by substrate in the ternary compex. X-Ray crystallographic results establishing the adenine nucleotide binding site, B_2R_2, together with the known ability of both adenine and adenosine to activate the enzyme in step II hydrolysis (Wieker and Witzel, 1967) suggest the activation is due to the binding of the adenosine moiety of 5′-AMP in the B_2R_2 site. This further suggests that the adenosine may be holding His-119 in position IV, and that this position may be correct for His-119 in step II as well as step I catalysis.

Acknowledgments

We thank Drs. Jeremy Knowles, Richard Henderson, Harold Wyckoff, and James Prestegard for their enthusiasm and willingness to discuss this work. We thank Drs. J. W. Faller and M. Saunders for their help with the operation of the HA-100 spectrometer and for use of the H-P function generator. We also thank Dr. J. S. Cohen for communicating pmr titration results prior to publication.

References

Anderson, D. G., Hammes, G. G., and Walz, F. G., Jr. (1968), *Biochemistry 7*, 1637.

Barnard, E., and Ramel, A. (1962), *Nature (London) 195*, 243.

Brocklehurst, K., Crook, E. M., and Wharton, C. W. (1967), *Chem. Commun. 924*, 63.

Brown, D. M., and Todd, A. R. (1953), *J. Chem. Soc.*, 2040.

Carlson, W. D., *et al.*, quoted in Richards and Wyckoff, 1971, to be published.

Cohen, J. S., Shrager, R. I., McNeel, M., and Schechter, A. N. (1970), *Biochem. Biophys. Res. Commun. 40*, 144.

Crook, E. M., Mathias, A. P., and Rabin, B. R. (1960), *Biochem. J.*, 234.

Dawson, R. M. C., Elliott, D., Elliott, W. H., and Jones, K. M. (1969), Data for Biochemical Research, 2nd ed, Oxford, Oxford Univ. Press.

Deavin, A., Fisher, R., Kemp, C. M., Mathias, A. P., and Rabin, B. R. (1968), *Eur. J. Biochem. 7*, 21.

Eadie, G. S. (1942), *J. Biol. Chem. 146*, 85.

Erman, J. E., and Hammes, G. G. (1966), *J. Amer. Chem. Soc. 88*, 5607.

Gassen, H. G., and Witzel, H. (1967), *Eur. J. Biochem. 1*, 36.

Glascoe, P. K., and Long, F. A. (1960), *J. Phys. Chem. 64*, 188.

Haffner, P. H. (1972), Ph.D. Thesis, Yale University.

Hammes, G. G., and Walz, F. G., Jr. (1969), *J. Amer. Chem. Soc. 91*, 7179.

Herries, D. G., Mathias, A. P., and Rabin, B. R. (1962), *Biochem. J. 85*, 127.

Hummel, J. P., Ver Ploeg, D. A., and Nelson, C. A. (1961), *J. Biol. Chem. 236*, 3168.

Hummel, J. P., and Witzel, H. (1966), *J. Biol. Chem. 241*, 1023.

King, N. L. R., and Bradbury, J. H. (1971), *Nature (London) 229*, 404.

Laidler, K. J. (1958), The Chemical Kinetics of Enzyme Action, London, Oxford University Press, p 87.

Meadows, D. H., and Jardetsky, O. (1969), *Proc. Nat. Acad. Sci. U. S. 61*, 406.

Meadows, D. H., Jardetsky, O., Epand, R. M., Ruterjans, H. H., and Scheraga, H. A. (1968), *Proc. Nat. Acad. Sci. U. S. 60*, 766.

Meadows, D. M., Markley, J. L., Cohen, J. S., and Jardetsky, O. (1967), *Proc. Nat. Acad. Sci. U. S. 58*, 1307.

Meadows, D. H., Roberts, G. C. K., and Jardetsky, O. (1969), *J. Mol. Biol. 45*, 497.

Myer, Y. P., and Schellman, J. A. (1962), *Biochim. Biophys. Acta 55*, 361.

Richards, F. M., and Wyckoff, H. W. (1971), *in* The Enzymes, Boyer, P. D., Lardy, H., and Myrbäck, K., Ed., 3rd ed, Vol. IV, New York and London, Academic Press.

Ruterjans, H., and Witzel, H. (1969), *Eur. J. Biochem. 9*, 118.

Schechter, A. N., Sachs, D. H., Heller, S. R., Shrager, R. I., and Cohen, J. S. (1973), *J. Mol. Biol.* (in press).

Schweizer, M. P., Broom, A. D., Ts'o, P. O. P., and Hollis, D. P. (1968), *J. Amer. Chem. Soc. 90*, 1042.

Smith, M., Moffatt, J. G., and Khorana, H. G. (1958), *J. Amer. Chem. Soc. 80*, 6204.

Ts'o, P. O. P., Melvin, I. S., and Olson, A. C. (1963), *J. Amer. Chem. Soc. 85*, 1289.

Van Holde, K. E., and Rossetti, G. P. (1967), *Biochemistry 6*, 2189.

Westheimer, F. H. (1968), *Accounts Chem. Res. 1*, 70.
Wieker, J. H., and Witzel, H. (1967), *Eur. J. Biochem. 1*, 251.
Wigler, P. W. (1968), *Biochem. Prep. 12*, 107.
Wilkinson, G. N. (1961), *Biochem. J. 80*, 324.
Witzel, H., and Barnard, E. A. (1962), *Biochem. Biophys. Res. Commun. 7*, 295.

Kinetics of Refolding of Guanidine Hydrochloride Denatured Cytochrome *c*. Temperature Dependence†

Robert W. Henkens* and Stephen R. Turner

ABSTRACT: Horse heart ferricytochrome *c* is denatured by guanidine hydrochloride and refolds upon removal of the denaturing conditions. The circular dichroism of the native and refolded protein is virtually identical, indicating that secondary structure and dissymmetrical interactions of heme and chromophoric side chains are recovered on refolding. Ikai and Tanford (Ikai, A., and Tanford, C. (1971), *Nature (London) 230*, 100) have recently reported kinetic evidence for the mechanism $N \rightleftharpoons X_1 \rightleftharpoons D \rightleftharpoons X_2$, in which the reversible interconversion of the native (N) and denatured (D) states involves two intermediates (X_1 and X_2). The intermediate X_2 is interpreted as representing an incorrectly folded form. Under the conditions of our experiments (25°, 2 M guanidine hydrochloride, pH 6.5), the first step in the ultimate conversion of D to N is the rapid formation of the incorrectly folded form. The absorbance changes associated with this step indicate that X_2 is highly folded. The temperature dependence of the rate constant for this step, $D \rightarrow X_2$, corresponds to the activation parameters $\Delta H^{\pm} = 15$ kcal mol^{-1} and $\Delta S^{\pm} = -6$ cal deg^{-1} mol^{-1}. Depletion of the incorrectly folded state and ultimate conversion of all the protein to the native state occur with apparent activation parameters of $\Delta H^{\pm} = 8$ kcal mol^{-1} and $\Delta S^{\pm} = -38$ cal deg^{-1} mol^{-1}. This shows that an unfavorable entropy change is a major barrier to conversion of the incorrectly folded form to N.

Cytochrome *c* is a small compactly folded protein molecule, consisting of a single polypeptide chain with no disulfide cross-links. The structure of crystalline horse heart ferricytochrome *c* has been determined by X-ray methods to a resolution of 2.8 Å (Dickerson *et al.*, 1971). In a detailed study of the kinetics of the reversible denaturation of this protein by guanidine hydrochloride, Ikai *et al.* (1973) report observations consistent with the view that transformation of the disordered polypeptide to the native protein involves rapid formation of a relatively highly ordered but incorrectly folded state; depletion of this incorrectly folded state and ultimate conversion of all the protein to the native state occur more slowly. We report here studies of the temperature dependence of the kinetics of refolding of horse heart ferricytochrome *c*. Activation parameters, $\Delta H^{\pm}$ and $\Delta S^{\pm}$, associated with the conversion of the random coil to the incorrectly folded form and with the conversion of the incorrectly folded form to the native protein, are deduced from these studies.

Experimental Section

Horse heart ferricytochrome *c*, crystalline protein type VI, was purchased from Sigma. Protein concentrations were determined from the absorbance at 550 nm, after reduction with sodium dithionite, using a molar absorptivity $\epsilon_{550} = 27.7 \times 10^4$ M^{-1} cm^{-1} (Margoliash and Frohwirt, 1959). Guanidine hydrochloride was purchased from Heico Inc. (Delaware Water Gap, Pa.). Guanidine hydrochloride stock solution concentrations were determined from the refractive index. All solutions were prepared with deionized water provided by Continental Water which had been filtered through a 0.45-μm Gelman membrane.

Spectral measurements were made with a Cary 15 spectrophotometer, periodically checked for absorbance linearity and excessive stray light, and a Durrum-Jasco J-15, standardized with *d*-10-camphorsulfonic acid using a specific ellipticity $[\psi]_{290} = 3.00 \times 10^3$ deg cm^3 g^{-1} dm^{-1}.

Fast kinetic measurements were made with a Durrum-Gibson stopped flow spectrophotometer. In most cases the optical pathlength was 2 mm, although in a few instances we used 2 cm to obtain data over a wider concentration range. The instrument is prone to a number of flow and optical artifacts, detected as anomalous transmittance changes in mixing experiments, and in actual kinetic experiments (*cf.* Ikai, 1971; Turner, 1971). We frequently checked for instrument error by mixing water with water and water with cytochrome *c* solution. Most of the errors could be detected by these simple mixing experiments, and were usually eliminated by removing trapped bubbles or realigning the optical system. In our experiments the reactant solutions differed markedly in refractive index. In the Durrum instrument, local refractive index gradients persist after mixing. This gives rise to Schlieren effects which cause oscillations in the transmittance. We found that working with shorter pathlengths and higher protein concentrations tended to reduce these oscillations to negligible proportions. Reaction solutions were degassed under house vacuum to reduce bubble formation during mixing. All components of the flow system were constructed of Kel F, Teflon, or glass. Temperature control was pro-

† From the Paul M. Gross Chemical Laboratory, Department of Chemistry, Duke University, Durham, North Carolina 27706. *Received August 24, 1972.* This work was aided by a Biomedical Science Support Grant from the National Institutes of Health to Duke University, and by funds from the National Science Foundation (GB-36050) and the Duke Endowment.